

Geological and Geochemical Record of 3400-Million-Year-Old Terrestrial Meteorite Impacts

DONALD R. LOWE, GARY R. BYERLY, FRANK ASARO, FRANK J. KYTE

Beds of sand-sized spherules in the 3400-million-year-old Fig Tree Group, Barberton Greenstone belt, South Africa, formed by the fall of quenched liquid silicate droplets into a range of shallow- to deep-water depositional environments. The regional extent of the layers, their compositional complexity, and lack of included volcanic debris suggest that they are not products of volcanic activity. The layers are greatly enriched in iridium and other platinum group elements in roughly chondritic proportions. Geochemical modeling based on immobile element abundances suggests that the original average spherule composition can be approximated by a mixture of fractionated tholeiitic basalt, komatiite, and CI carbonaceous chondrite. The spherules are thought to be the products of large meteorite impacts on the Archean earth.

METEORITE IMPACTS PLAYED A fundamental role in the evolution of planetary surfaces in the early solar system. Although reflected in cratered terranes on many planets and satellites, this stage in terrestrial evolution has been lost through later crustal recycling. Recently discovered spherule layers in early Archean greenstone belts in South Africa and Western Australia, however, may provide a glimpse of the final stage of heavy bombardment (1, 2). In this report, we outline evidence that at least three spherule layers in the Barberton Greenstone belt, South Africa, represent distal ejecta or condensate blankets produced by large meteorite impacts on the early earth.

The 3500- to 3200-million-year-old Barberton Greenstone belt includes a lower, predominantly volcanic sequence, the Onverwacht Group, and an upper, mainly sedimentary sequence, the Fig Tree and Moodies groups (Fig. 1). The volcanic section, 8 to 10 km thick, is made up of mafic and ultramafic volcanic rocks, subordinate silicic volcanic units, and thin cherty sedimentary layers. The rocks accumulated as a flat, subsiding, predominantly shallow-water oceanic volcanic platform (3). The volcanic succession is overlain conformably by up to 6 km of predominantly volcanoclastic and orogenic sedimentary rocks of the Fig Tree

and Moodies groups. These strata range from mainly terrestrial and shallow-water units in southern parts of the belt to deep-water marine units in the north. The entire succession was deposited between 3550 and 3200 million years ago (Ma) (4), and the volcanic-sedimentary transition occurred at about 3400 Ma.

Spherule beds occur in both the volcanic and sedimentary sequences (Fig. 1). The lowest, S1, has not been studied and is not discussed further. Beds S2, S3, and S4 are in the lowest part of the Fig Tree Group. They are made up largely of sand-sized spherules, mostly 0.1 to 4 mm in diameter (Fig. 2), composed mainly of intergrown microcrystalline quartz, sericite, chlorite, opaque oxides, and carbonate.

The lowest of the Fig Tree beds, S2, ranges from a few centimeters to over 1 m thick, occurs in the basal 1 to 3 m of Fig Tree strata, and is present across virtually the entire greenstone belt. It represents a regionally synchronous depositional event and is an important horizon for stratigraphic correlation. Bed S3, 20 to 140 cm thick, crops out 50 to 250 m above S2 and has been identified with certainty only in southern areas. In northern sections, this part of the Fig Tree Group is composed largely of turbiditic graywacke, and S3, if deposited, would be difficult to locate in this 2000-m-thick clastic sequence. To date, bed S4, 10 to 15 cm thick and located 6 m above S3, has been identified in only a single outcrop in the southern part of the belt. Like S3, it is interbedded in a thick, poorly resistant sequence of clastic rocks and may be considerably more widespread.

Many rocks in the Barberton sequence have been metasomatically altered, including the spherule beds, which show evidence of carbonation and silica and potash metasomatism (5). Primary immobile element ratios, however, especially among Al, Ti, Cr, V, Zr, and the rare earth elements (REE), are roughly preserved (6).

The compositional, textural, and geochemical properties of the spherule beds collectively provide compelling evidence that they represent distal debris blankets produced by meteorite impacts:

1) Spherules in S2 and S3 contain chert, mica, and oxide pseudomorphs after needle-shaped and barred skeletal crystallites that morphologically resemble quenched pyroxene and olivine microspinel in both komatiitic flow rocks and chondrules (1). These textures indicate that the spherules formed by the quenching of liquid silicate melts (Fig. 2). The common inward and edge-centered growth habits (1) indicate that the crystals grew after the droplets had assumed their spherical shapes. Geologic occurrences of natural silicate droplets include impact-produced, mainly distal deposits, such as Cretaceous-Tertiary (K-T) boundary units (7) and Eocene clinopyroxene spherule and microtektite layers (8), and ballistic debris aprons around lava fountains (9).

2) The layers occur as widespread sheets, are not interbedded with komatiitic or basal-

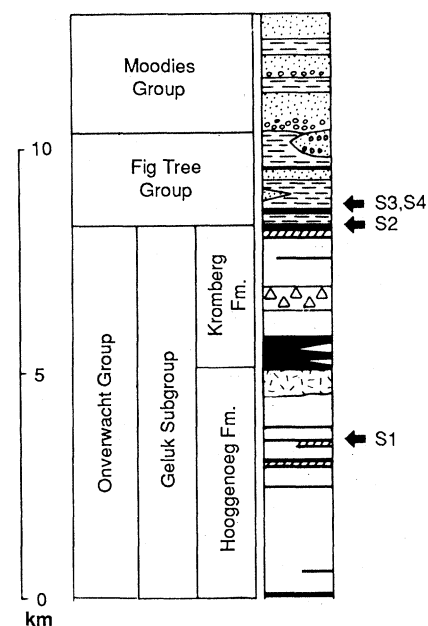


Fig. 1. Generalized stratigraphic column of the upper part of the Swaziland Supergroup, Barberton Greenstone belt, South Africa, showing positions of spherule beds. Symbols: mafic and komatiitic volcanic rocks (white); dacitic volcanic rocks (random line segments); altered komatiitic volcanic rocks (cross hatching); cherts (black); shale (horizontal line segments); sandstone (stipple); and conglomerate (open circles). Fm, Formation.

D. R. Lowe, Department of Geology, Stanford University, Stanford, CA 94305.
G. R. Byerly, Department of Geology and Geophysics, Louisiana State University, Baton Rouge, LA 70803.
F. Asaro, Lawrence Berkeley Laboratory, University of California, Berkeley, CA 94720.
F. T. Kyte, Institute of Geophysics and Planetary Physics, University of California, Los Angeles, CA 90024.

tic volcanic rocks, and lack juvenile volcanic and volcanoclastic components. The confirmed outcrop area of S2 is at least 20 by 50 km, and new discoveries may extend this distribution to the present outcrop limits of the Fig Tree Group. With structural restoration, the original area represented by the S2 outcrops was at least 30 by 100 km. This area greatly exceeds the expected dispersal area of liquid droplets thrown out during lava fountaining.

3) The spherule beds were deposited as blankets across all existing surficial environments and depositional settings, including (i) deep- and shallow-water, (ii) current-active and quiet water, and (iii) clastic-choked, orthochemical, and biologically dominated environments. The composition and structuring of the spherule beds are directly related to the local depositional settings into which the spherules fell (2). In relatively deep-water areas and some protected shallow-water areas, spherules accumulated directly as fall deposits, and these rocks consist almost entirely of spherules and lack mixed detrital debris and evidence for current deposition. In shallow-water settings, the spherules were commonly reworked by currents and mixed with unrelated clastic grains.

4) The heterogeneous compositions of spherules mixed in S2 and S3 rule out simple eruptive or magmatic origins. One section of S3, 38 cm thick, includes compositionally and texturally distinctive lower and upper divisions (1). The lower part of

the bed is composed of a bimodal mixture of large high-silica spherules up to about 3 mm in diameter and smaller high-alumina spherules generally less than 1 mm in diameter, both lacking quench textures (Fig. 2A). The upper part of the same bed consists of a diverse population of spherules, 0.8 to 2 mm in diameter, composed of intergrown chert, sericite, and chlorite (Fig. 2B). Spherules near the top of the bed show well-developed quench textures, and many contain central cavities now filled by chert or druzey quartz; this texture indicates that they were originally hollow.

Spherules in S4 are composed entirely of structureless microcrystalline chlorite lacking quench textures or any other evidence for the former presence of primary mineral grains. These spherules were probably composed originally of amorphous silicate glass.

5) The spherule layers are sites of extreme Ir enrichment (10) (Table 1). Bed S4 has a measured bulk-bed Ir concentration of 162 ppb (Table 1). One 7.5-cm-thick sample across most of S4 was cut into 15 0.5-cm-thick slices parallel to bedding. Measured Ir was from 7 to 361 ppb, and four slices had Ir concentrations greater than 200 ppb. Thus, Ir is heterogeneously distributed at a scale of 0.5 cm. Interbedded clastic sedimentary units have Ir levels below 0.5 ppb. Spherule layers S2 and S3 have yielded maximum Ir concentrations of 76 and 145 ppb, respectively, in fall-deposited facies. In most southern sections, these layers were reworked by currents following deposition,

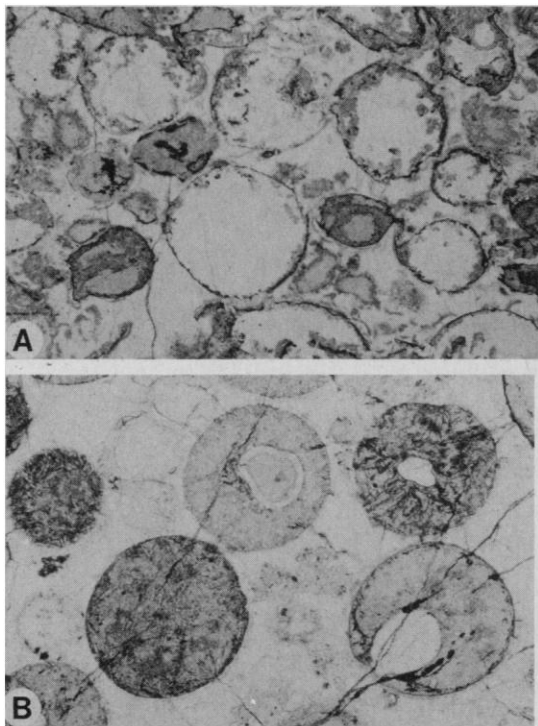


Fig. 2. Spherules from S3, section SAF-206. (A) Lower part of 38-cm-thick bed with bimodal spherule mixture. Larger spherules, reaching 2 mm in diameter in photo, are composed of nearly pure microcrystalline silica (white) rimmed by microcrystalline sericite (gray) and iron oxides (black). Smaller spherules, 0.5 to 1.0 mm in diameter, are composed of sericite or chlorite with up to 45 weight percent Al_2O_3 , or both. Most spherules show some postdepositional compression. (B) Upper part of same bed. Larger spherules are 1.0 mm in diameter and composed of microcrystalline silica and sericite. Three darker spherules show well-developed quench textures. The two lighter spherules contain deformed, filled central cavities. Faint, smaller silica spherules occur locally between the larger spherules.

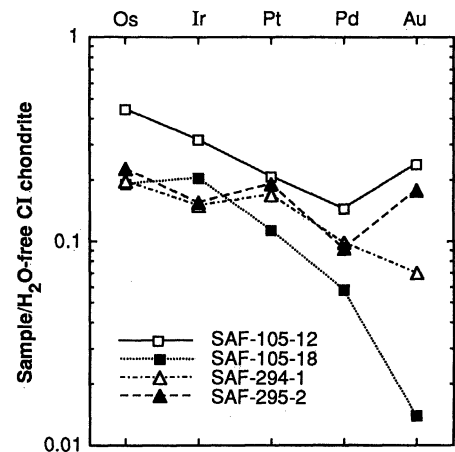


Fig. 3. Abundances of Os, Ir, Pt, Pd, and Au in samples of spherule beds S2 and S3. Samples are normalized to H_2O -free CI chondrites (17). The flat patterns for three samples indicate a close similarity to noble metal abundances in chondritic meteorites.

and the spherules were winnowed and mixed with unrelated clastic particles. The Ir contents of such rocks generally average between 0.4 and 5 ppb (Table 1).

Associated country rocks in the greenstone belt have much lower Ir concentrations (Table 1). The highest measured Ir concentration in any rock except the spherule layers was 4.9 ppb in a komatiitic basalt, a reasonable upper value for komatiites (11). All dacites and sedimentary rocks other than the spherule layers contained less than 0.5 ppb Ir (Table 1).

The measured Ir concentrations, particularly in S4, are comparable to or greater than those reported in typical K-T boundary clays, which commonly have Ir maxima between 10 and 60 ppb (12-14). However, individual samples of K-T boundary sediments from Stevns Klint, Denmark, and Woodside Creek, New Zealand, contain as much as 120 and 460 ppb Ir, respectively, on a carbonate-free basis (14, 15).

6) Analyses of other noble metals in a number of samples by radiochemical neutron activation analysis indicate that S2 and S3 are also enriched in Pd, Os, Pt, and Au (16) in roughly chondritic proportions (Fig. 3). Three of the four samples analyzed have noble metal abundances similar to those of CI chondrites (17). In most cases, ratios between individual noble metals and Ir are within a factor of 2 of chondritic ratios and the mean ratio for all samples is 0.82 times chondritic.

7) Although most Barberton rocks, including the spherule layers, have been profoundly altered by early low-temperature metasomatism, relict primary spinels are trace constituents in most samples. In S2 and S3, spinels occur in mica-rich spherules,

and the abundance of these spherules correlates directly with the Ir contents of the samples. Spinels do not occur in S4. Microprobe analysis indicates that Cr in S4 spherules is in solid solution in chlorite. The absence of detectable minerals other than

Table 1. Measured maximum and averaged concentrations of iridium in rocks and spherule layers in the Barberton Greenstone belt, South Africa. Analyses as in (10) except where indicated; uncertainties represent instrumental errors.

Sample	Ir (ppb)
<i>Komatiitic volcanic rocks*</i> †	
SA106-1	4.9 +1.1/-0.9
SA73-2	2.3 +0.8/-0.6
SA106-2	1.5 +0.7/-0.5
SA72-4	1.3 +0.7/-0.5
SA224-7	1.3 +/-0.2
Mean of 14	1.4
<i>Silicified komatiitic ash and sandstone</i>	
SAF-10-12	1.6 +0.5/-0.4
SAF-358-1	1.4 +0.5/-0.4
SAF-186-1	0.50 +0.39/-0.24
Mean of 5	0.8
<i>Dacitic volcanic rocks‡</i>	
SA31-3	0.09 +0.27/-0.09
Mean of 4	0.02
<i>Dacitic tuff and silicified ash</i>	
SA37-3	0.41 +0.40/-0.22
SAF-295-5	0.34 +0.34/-0.19
SAF-105-30	0.25 +0.29/-0.16
Mean of 10	0.18
<i>Shale§</i>	
SAF-23-314	0.28 +0.33/-0.18
SAF-294-5	0.22 +0.29/-0.14
SAF-296-5	0 +0.25
<i>Jasper§</i>	
SAF-17-1	0.20 +0.36/-0.17
SAF-296-3	0 +0.19
<i>Barite§</i>	
SAF-240-5	0.33 +0.95/-0.33
<i>Black carbonaceous chert </i>	
SAF-295-9	0.32 +0.31/-0.18
SAF-357-9-3	0.16 +0.34/-0.16
SAF-244-1	0.10 +0.23/-0.08
Mean of 6	0.12
<i>Graywacke and sandstone§</i>	
SAF-296-4	0.21 +0.31/-0.15
SAF-244-6	0.20 +0.27/-0.13
SAF-230-4	0 +0.19
<i>S2, northern areas</i>	
SAF-295-2	75.9 +/-3.4
SAF-294-1	66.6 +/-3.4
SAF-357-9-1	4.5 +/-0.8
<i>S2, southern areas</i>	
SAF-105-23	1.6 +0.61/-0.46
<i>S3</i>	
SAF-105-12-3¶	144.5 +/-5.1
SAF-105-18¶	96.4 +/-4.1
SAF-105-15¶	11.2 +/-1.2
SAF-227-3	5.8 +/-0.9
<i>S4</i>	
SAF-349-3	52.6 +/-2.3
SAF-179-15	162 +/-6

*Measured against flux monitor of ¹⁵²Eu. †All samples from uppermost 1000 m of Onverwacht Group. ‡Schoongezicht Formation, upper unit of Fig Tree Group. §Lower part of Fig Tree Group. ||Uppermost Onverwacht Group, 1 to 5 m below S2. ¶Subsamples of S3 from the same locality.

chlorite and the direct correlation between Cr and Ir concentrations in S4 samples suggests that the Ir is also contained in solid solution in the chlorite.

Spinels in the S2 and S3 are chemically distinct from those in komatiites and virtually all other known volcanic rocks (6). The spinels in S2 and S3 have low concentrations of Al, Mg, and Ti, typically below 1 weight percent, and very high concentrations of NiO (to 17%), ZnO (to 5%), and V₂O₅ (to 2%). Both spherule layers and komatiites show a direct correlation between Cr and Ir abundances (Fig. 4) but have significantly different Cr/Ir ratios. These relations suggest that spinels are the Ir carriers in these units but also that the spinels in each unit have different petrogenetic origins. The Barberton spherule-bed spinels are similar to spinels in K-T spherules in containing low Ti and high Ni contents (18), a feature which distinguishes both from most terrestrial spinels, but contrast with K-T spinels in also having low Al and Mg.

Collectively, these observations provide strong evidence that the Early Archean spherule layers are not products of normal igneous or sedimentary processes. Although unknown exotic terrestrial mechanisms of formation cannot be dismissed, available evidence is most consistent with spherule formation through large Archean impacts. The data rule out an origin by erosion of underlying portions of the greenstone belt, as has been proposed (19). Firstly, spherules are confined to the described spherule beds. If they formed as detrital components, such as amygdules or varioles eroded from mafic or komatiitic volcanic rocks (19), they should be present in clastic units throughout the sequence, which contain abundant komatiitic and basaltic detritus. Hydraulically, there is no known natural mechanical sedimentary process that could concentrate spherical grains with quench textures to the complete exclusion of hydraulically equivalent irregular detrital particles, which make up interbedded clastic layers. Furthermore, where the beds are composed entirely of spherules, they lack current structures; where they contain current structures, they generally contain less than 10% spherules. Hence, mechanical working by currents tended to dilute, not concentrate, spherules. Finally, the Ir abundances and spinel geochemistries in the spherule beds are unlike those in associated volcanic units, precluding an origin through simple erosion.

An estimate of the average composition of spherules in S2 and S3, based on immobile-element composition as determined by bulk rock x-ray fluorescence analyses of the spherule layers and microprobe analyses of

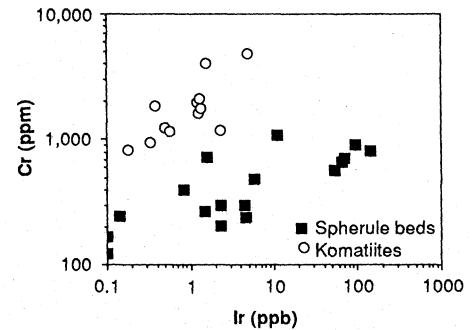


Fig. 4. Chromium and Ir compositions of spherule layers and komatiites from Barberton belt. Microprobe as well as x-ray fluorescence and petrographic analyses indicate that Cr in both rock types is contained mainly in chrome spinels. The direct relation between Cr and Ir in both suggests that much of the Ir is also contained in spinels. The contrasting Cr-Ir relations between komatiites and spherule layers reflect compositional differences between spinels in each, indicating that spherule-layer spinels are not recycled igneous spinels.

quench-textured spherules, seems to be internally consistent and reflects a mixed source consisting of both target and impactor rocks, predominantly basalt (70 to 80%), but including small amounts of komatiite and chondritic materials (6). Bed S4, averaging about 160 ppb Ir and nearly 1000 ppm Cr, is considerably more mafic in composition and may include up to 30% chondritic components.

Silt-sized and finer airborne dust-sized debris produced by the impacts may be present in or above the spherule beds but would be difficult to distinguish petrographically because of alteration and, in current-deposited units, mixing with clastic particles. The lack of primary quartz and other appropriate unaltered primary mineral grains in the spherule layers precludes identification of shocked minerals.

If the spherule layers formed as distal meteorite-impact debris blankets, they provide the first tangible terrestrial record of the Archean bombardment history of the earth. The great thickness of the Archean spherule layers compared to that of known younger spherule and microtektite deposits suggests that the Archean impactors were substantially larger than the younger projectiles. The absence of coarse ballistic ejecta in the fall-deposited facies of the beds suggests that the spherules may have formed by the condensation of an impact-produced vapor cloud representing both target rocks and projectile. The compositional heterogeneity of the spherules could thus have arisen as a result of changing composition of condensates in the cooling vapor cloud. The compositional and textural grading in the fall-deposited facies may reflect both the condensation sequence in the cooling vapor cloud and

hydraulic sorting of the spherules during fall.

O'Keefe and Ahrens (20) have argued that the radius of droplets condensing from impact-produced rock vapor clouds is a function of projectile diameter and, to a lesser extent, velocity. Spherules from the K-T boundary are invariably less than 1 mm in diameter. Based on their results [figure 22 in (18)], our largest spherules, about 3 mm in diameter, would correspond to projectiles between about 20 and 50 km in diameter.

Over virtually the entire Barberton belt, S2 lies within 1 m stratigraphically of the transition from volcanic to sedimentary stages of greenstone belt evolution. This lithologic break marks a profound tectonic, sedimentological, and petrologic change in the history of the Barberton belt. Its coincidence with S2 may be just that, a fortuitous coincidence of unrelated events, or it may indicate that major tectonic and crust-forming events on the early earth were controlled or strongly influenced by meteorite impacts.

REFERENCES AND NOTES

1. D. R. Lowe and G. R. Byerly, *Geology* **14**, 83 (1986).
2. ———, *Lunar Planet. Sci.* **XIX**, 693 (1988).
3. D. R. Lowe and L. P. Knauth, *J. Geol.* **85**, 699 (1977); D. R. Lowe, *Precamb. Res.* **17**, 1 (1982).
4. A. R. Tagtmeyer and A. Kroner, *ibid.* **36**, 1 (1987); A. Kroner and W. Compston, *ibid.* **38**, 367 (1988).
5. K. C. Duchac, thesis, Louisiana State University, Baton Rouge (1986); ——— and J. S. Hanor, *Precamb. Res.* **37**, 125 (1987); D. R. Lowe and G. R. Byerly, *Nature* **324**, 245 (1986).
6. G. R. Byerly, D. R. Lowe, F. Asaro, *Lunar Planet. Sci.* **XIX**, 152 (1988).
7. M. Montanari *et al.*, *Geology* **11**, 668 (1983); spherules are nearly ubiquitous in K-T boundary sediments. In most cases, their mineralogy is clearly authigenic; therefore, their origins are commonly disputed. However, probable primary minerals have been identified in some spherules: spinels by J. Smit and F. T. Kyte [*Nature* **310**, 403 (1984)] and clinopyroxene by J. Smit *et al.* [paper presented at the Conference on Global Catastrophes in Earth History, 20 to 23 October, Snowbird, Utah (Lunar and Planetary Institute, Houston, TX, 1988), p. 182].
8. C. John and B. P. Glass, *Geology* **2**, 599 (1974); B. P. Glass, C. A. Burns, J. R. Crosbie, D. L. DuBois, *J. Geophys. Res.* **90**, D175 (1975).
9. G. Heiken and D. McKay, *Proc. Lunar Sci. Conf.* **8**, 3243 (1977); *Proc. Lunar Planet. Sci. Conf.* **9**, 1933 (1978).
10. D. R. Lowe, F. Asaro, G. R. Byerly, *Lunar Planet. Sci.* **XIX**, 695 (1988). Most Ir measurements were made by F.A. with the Ir Coincidence Spectrometer (ICS) at Lawrence Berkeley Laboratory, University of California. The ICS measures Ir abundance following neutron activation by determining the coincidence between two gamma rays of ^{192}Ir using twin Ge crystals.
11. J. H. Crocket, *Can. Mineral.* **17**, 391 (1979); R. R. Keays, in *Komatites*, N. T. Arndt and E. G. Nisbet, Eds. (Allen and Unwin, London, 1982), pp. 435–457.
12. L. W. Alvarez, W. Alvarez, F. Asaro, H. V. Michael, *Science* **208**, 1095 (1980).
13. R. Ganapathy, *ibid.* **216**, 885 (1982); W. Alvarez, F. Asaro, H. V. Michael, L. W. Alvarez, *ibid.*, p. 886 (1982).
14. F. T. Kyte, Z. Zhou, J. T. Wasson, *Nature* **288**, 651 (1980).

15. B. Schmitz, *Geology* **16**, 1068 (1988).
16. F. T. Kyte, D. R. Lowe, G. R. Byerly, *Meteoritics* **23**, 284 (1988).
17. E. Anders and M. Ebihara, *Geochim. Cosmochim. Acta* **46**, 2363 (1982).
18. F. T. Kyte and J. Smit, *Geology* **14**, 485 (1986).
19. R. Buick, *Geology* **15**, 180 (1987); M. J. de Wit, *Lunar Planet. Sci.* **XVII**, 182 (1986).
20. J. D. O'Keefe and T. J. Ahrens, *Geol. Soc. Am. Spec. Pap.* **190**, 103 (1982).
21. This research has been supported by grant no. NAGT 9-136 from the Early Crustal Genesis Project, Planetary Materials Division, National Aero-

navics and Space Administration to D.R.L. and G.R.B.; NSF grant no. EAR-8406420 to D.R.L.; U.S. Department of Energy contract DE-AC03-76SF00098 and NASA contract A-59508C to F.A.; and Office of Naval Research grant N00014-87 to F.T.K. We are also grateful to A. K. Knowles, Anglo-American Corp.; R. Rossiter, Gencor Mining; Anglo Vaal Mining Company; ETC Mines; and the Department of Geology, University of the Witwatersrand for providing field support and property access.

7 April 1989; accepted 30 June 1989

Silicon Coordination and Speciation Changes in a Silicate Liquid at High Pressures

XIANYU XUE, JONATHAN F. STEBBINS, MASAMI KANZAKI, REIDAR G. TRØNNES

Coordination and local geometry around Si cations in silicate liquids are of primary importance in controlling the chemical and physical properties of magmas. Pressure-induced changes from fourfold to sixfold coordination of Si in silicate glass samples quenched from liquids has been detected with ^{29}Si magic-angle spinning nuclear magnetic resonance spectrometry. Samples of $\text{Na}_2\text{Si}_2\text{O}_5$ glass quenched from 8 gigapascals and 1500°C contained about 1.5 percent octahedral Si, which was demonstrably part of a homogeneous, amorphous phase. The dominant tetrahedral Si speciation in these glasses became disproportionated to a more random distribution of bridging and nonbridging oxygens with increasing pressure.

INFORMATION ABOUT THE STRUCTURE of liquid silicates is necessary for understanding the bulk chemical and physical properties of magmas. The best known and most fundamental aspect of this structure is the regular coordination of Si by four O atoms (Si^{IV}). All evidence indicates that at ambient pressure for geologically important compositions, Si^{IV} predominates in silicate melts and glasses, as it does in crystalline minerals (1).

At the pressures that are present throughout most of the earth's interior, on the other hand, Si in crystalline silicates is evidently six-coordinated (Si^{VI}), and the transition to the higher coordination occurs between 8 and 25 GPa (about 240- to 750-km depth) (2). Analogous transitions from Si^{IV} to Si^{VI} in silicate liquids have been postulated to account for high-pressure phase equilibria and liquid densities and viscosities (3) and were predicted from molecular dynamic simulations (4). However, direct spectroscopic evidence for Si^{IV} in high-pressure liquid silicates is limited. Both Raman and infrared absorption spectroscopy on silicate glasses at room temperature and pressures to

nearly 40 GPa have demonstrated that significant structural changes do occur (5). The infrared data have been interpreted as indicating the disappearance of well-ordered SiO_4 tetrahedra and the formation of species with higher coordinations, but the Raman data showed no clear evidence for Si^{IV} . However, these results may not be directly applicable to equilibrium liquids because such liquids have much higher thermal energies than glasses at room temperature, possibly allowing additional mechanisms of structural response to pressure.

The development of large volume high-pressure apparatus has allowed samples of up to 10 mg to be synthesized at pressures to 25 GPa and temperatures above 2000°C (6) then rapidly quenched for spectroscopic work at ambient conditions. The structure of a quenched glass is generally assumed to record that of the equilibrium liquid at its glass transition temperature (T_g), although some local displacive change may take place during decompression (5). A coordination increase for Al^{3+} (structurally analogous to Si^{4+}) has been reported in a ^{27}Al NMR (nuclear magnetic resonance) study of such samples (7). Recent solid-state ^{29}Si NMR work has demonstrated that the technique is useful in detecting and characterizing both Si^{IV} and Si^{VI} (8), as well as for distinguishing amorphous from crystalline materials. We have applied this technique to find

X. Xue, M. Kanzaki, R. G. Trønnnes, C. M. Scarfe Laboratory of Experimental Petrology, Department of Geology and Institute of Earth and Planetary Physics, University of Alberta, Edmonton, Canada T6G 2E3. J. F. Stebbins, Department of Geology, Stanford University, Stanford, CA 94305.